EPD Congress 2006 *Edited by S.M. Howard, R.L. Stephens, C.J. Newman, J.-Y.J. Hwang, A.M. Gokhale, T.T. Chen, T.P. Battle, M.L. Free, B.R. Davis, C.L. Harris, H. Henein, P.N. Anyalebechi, A.C. Powell, G.K. Krumdick, and C.K. Belt*
TMS (The Minerals, Metals & Materials Society), 2006

The Characterization of the Intermetallic Fe-Al Layer of Steel-Aluminum Weldings

M. Potesser[1], T. Schoeberl[2], H. Antrekowitsch[1] and J. Bruckner[3]

[1]University of Leoben – Department Metallurgy – Nonferrous Metallurgy
8700 Leoben, Austria

[2]University of Leoben, Erich Schmid Institute and Department of Material physics
8700 Leoben, Austria

[3]Fronius International GmbH.
4600 Wels, Austria

Keywords: FeAl3, FeAl, Fe2Al5, intermetallic phase, less heat input; less spatter; new kind of droplet, detachment in MIG – technology, atomic force microscopy, nanointending

Abstract

One of the main targets in the automotive mass industry and supplying industry is the weight reduction of the vehicle for decrease of the fuel consumption. For that reason combinations of different kinds of materials and connections of, for example, steel and aluminium are developed or are already successfully field-tested. A determining factor concerning the quality assessment of the welded joint during hybrid welding is the characterization of the intermetallic Fe-Al layer regarding strength, hardness, morphology and mainly the different phases in which Fe occurs together with the Aluminum (FeAl, Fe_2Al_5, $FeAl_3$.). A combination of conventional light microscopy, SEM - EDX - analysis, the usage of an atomic force microscope including a Nanoindenter and theoretical thermodynamic calculations turned out to be highly effective. Based on the attained results, the constitution of the intermetallic FeAl layer, influenced by silicon, manganese and zinc, can be predicted.

Introduction

Owing to the diversity of demands set to construction materials, it is, in many cases, necessary to create very unorthodox material combinations. One possibility of meeting these requirements is the joining of two materials. In some parts of the automotive industry, combinations of aluminum and steel have been increasingly applied in the past years. However, with regard to the differences in chemical and physical characteristics and the formation of brittle intermetallic phases (IMP), many problems arise. The combination of steel and aluminium is achieved by various welding methods, such as electron beam-, laser-, TIG-, MIG- and rubbing welding. A new method, the CMT-process for joining of aluminum and steel, shows excellent performance with regard to the quality of the joining. The joining is established by combined effects of fusion and solid state welding (welding/brazing). The aim of this investigation was to find a connection between the alloy content, the structure of the intermetallic compounds and the strength properties of the IMP. The IMPs were determined through nanohardness measurement and thermodynamic calculations.

Basics of the IMPs in the Fe-Al phase diagram

When joining materials, thermal conductivity, differences in the melting points and solubilities of the materials with each other play an important role for the mechanical characteristics of the resulting joining. The combinations of Al and Fe and Al and Ti are significant for industrial applications. According to the specific material properties, there is a large difference between melting points and thermal conductivities of these material combinations which lead to severe problems during joining with conventional welding technologies such as MIG and TIG. These subsequent problems are the formation of IMPs and crack formation within the joint zone with subsequent failure of the joining[1], [2].

The Fe-Al equilibrium phase diagram is shown in Figure 1, the IMP with allowable mechanical properties in case of weldings is marked. The system is characterized with an iron-based solid solution and six non-stoichiometric intermetallic compounds of Fe_3Al, FeAl (α_2), $FeAl_2$, Fe_2Al_3 (ε), Fe_2Al_5 and $FeAl_3$. Table 1 indicates crystal structure, stability range and hardness for this phase diagram with special emphasis on the IMPs [5]-[7].

Several studies focusing on the microstructural analysis of the interface layer of molten aluminum coming in contact with solid iron have been conducted [6], [8]-[15].

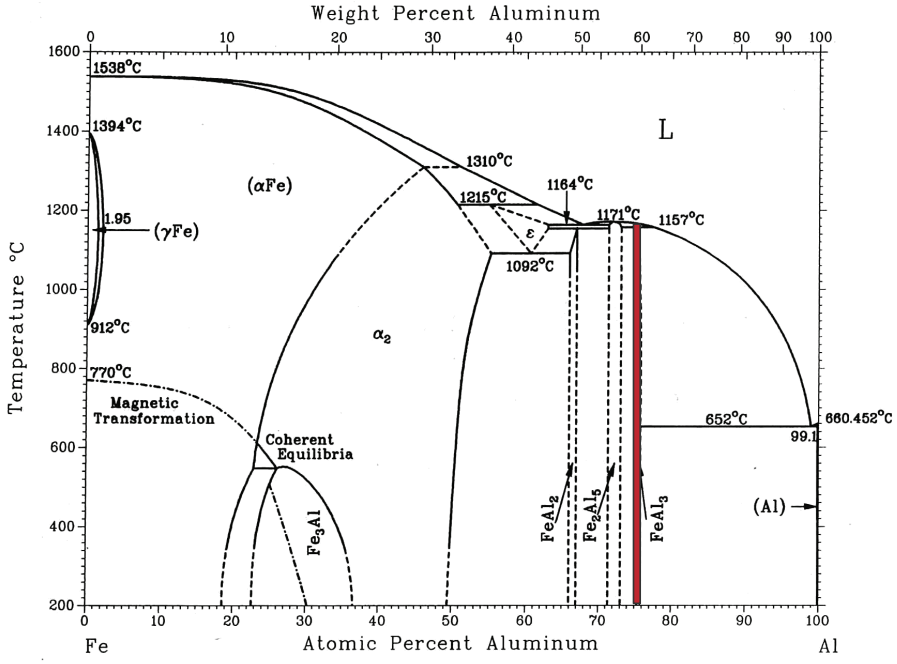

Figure 1: Fe-Al equilibrium phase diagram[5]

Table I: Crystal structure, stability range and hardness of the phases formed in Fe-Al binary System at room temperature [3]-[7]

Phases	Crystal structure	Stability range (at.%)	Vickers Hardness (9.8N)
Fe solid solution	BCC	0-45	not investigated
γ-Fe	FCC	0-1.3	not investigated
FeAl	BCC (Order)	23-55	470[3](491 – 667)[4]
Fe_3Al	DO3	23-34	330[3] (344 – 368)[4]
Fe_2Al_3	Cubic (complex)	58-65	not investigated
$FeAl_2$	Triclinic	66-66.9	unknown[3] (1058 – 1070)[4]
Fe_2Al_5	Orthorhombic	70-73	1013[3] (1000 – 1158)[4]
$FeAl_3$	Monoclinic	74.5-76.5	892[3] (772 – 1017)[4]
Al solid solution	FCC	99.998-100	not investigated

During thermal joining of dissimilar material combinations, the formation of IMPs plays a significant role. Depending on the process related temperature and time cycle, a severe IMP formation occurs. Together with the phase formation, an embrittlement of the joining zone can be observed. However, if material joinings with high toughness and strength are required, the IMP formation has to be limited to a minimum size. The main parameters are the limitation of the overall heat input and the reduction of melting pool dimensions. Under these considerations, laser joining provides an excellent tool for these technical demands. Due to the small spot diameter of laser beams, locally high energy densities are achieved, finally resulting in a significant improvement of joining speed and a reduction of the melt pool diameter. Due to the high thermal gradients during laser beam joining, the resulting rapid cooling of the melt pool also has a positive influence on the limited IMP formation. A further process with these properties is the CMT-Process.

The CMT-Process

The CMT (Cold Metal Transfer)-process is a revolution in welding technology, with respect to both, welding equipment and welding applications. The CMT-process is not only a completely new process-, unknown until now-, but it also opens a new field of application since it widens the limits of Gas Metal Arc Welding (GMAW), allowing the arc joining of steel to aluminum in a reproducible manner for the first time.
This paper firstly describes the principle of the CMT-process in a very detailed way. Secondly, the properties and advantages of the process are shown. Thirdly, the welding system and the three main applications of the CMT-process are presented and illustrated with examples.

The history of the CMT-process

The CMT-process has a long history. In 1991 Fronius started research in the fields of arc joining of steel with aluminum. The breakthrough could be obtained with the CMT-process due to its low heat-input. The second source of the CMT-process is the spatter-free ignition SFI, where the wire is pushed towards and also pulled back from the work piece. For the first time in welding history, the wire was intentionally pulled back. Finally in 1999 a customer demanded welding only very few droplets of filler wire onto very thin sheets.
At that time the base for the development of the CMT-process was set. In 2002 the process itself was already quite well known and the project CMT started, which aim is the development of a welding equipment suitable for a industrial application of the CMT-process.

The principle of the CMT-process

CMT is the abbreviation for Cold Metal Transfer and describes a GMAW process whose heat-input is low as compared to the conventional dip arc process. This explains the word *Cold* in the process name. The CMT-process is a dip arc process with a completely new method of the droplet detachment from the wire.
In the conventional dip arc process the wire is moved forward until a short circuit occurs. At that moment the welding current rises, causing the short circuit to reopen, allowing the arc to ignite again. There are two main features of the CMT-process: On the one hand the high short circuit current corresponds to a high heat input. On the other hand the short circuit opens in a rather uncontrolled manner, resulting in lots of spatters in the conventional dip arc process. In the CMT-process the wire is not only pushed towards but also drawn back from the work piece – an oscillating wire feeding with an average oscillation frequency up to 70 Hz is used as it is shown in Figure 2.

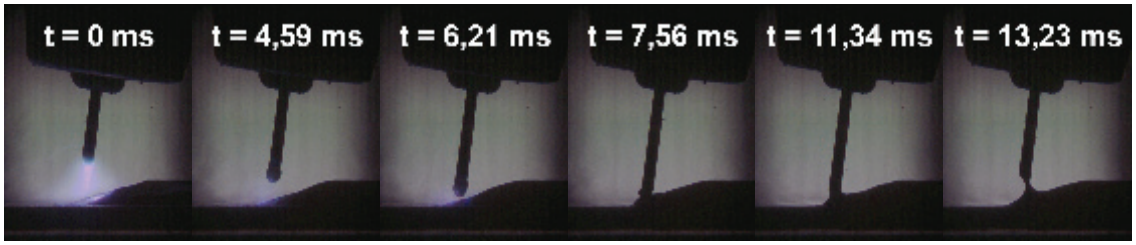

Figure 2: The principle of the CMT-process, where an oscillating wire feeding is performed.

There are three features of the CMT-process, which distinguish this process from a conventional GMAW process:
First of all, the wire movement is directly included into the welding process control. Until now the wire feed speed during welding was either fixed or had a predetermined time schedule (e.g. synchropulse). In the CMT-process the wire is moved towards the work piece until a short circuit occurs. At that moment the wire speed is reversed and the wire pulled back. When the short circuit opens again, the wire speed is again reversed, the wire moves towards the work piece again and the process begins again. There is no predetermined time schedule for the wire movement, but the occurrence and the opening of a short circuit determine the wire speed and direction. It can be said that there is an interaction between the processes in the welding pool and the wire movement. This is the reason why one can only speak of an average oscillation frequency of the wire, depending exactly on the occurrence of the short circuit. Therefore the oscillation frequency of the wire varies with time – averaging around 70 Hz.
The second feature which characterizes the CMT-process is the fact that the metal transfer is almost current-free, while the conventional dip arc process corresponds to a high short circuit current. In the CMT-process the current is no longer responsible for the opening of the short circuit. When the wire is drawn back, the movement supports the metal transfer due to the surface tension of the molten material. Therefore the current during the short circuit can be kept very low and the heat input is also very small. Figure 3 shows a schematic diagram of the current / voltage during the CMT-process:

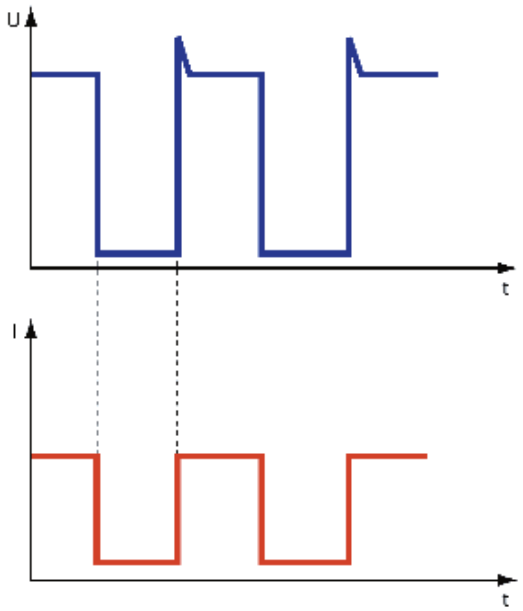

Figure 3: Schematic diagram of current and voltage during the CMT-process

Finally the CMT-process is characterized by the fact that the wire movement supports the metal transfer as mentioned above.

Investigated material combinations

Aluminum (5xxx and 6xxx) and steel sheets (low carbon steel with a zinc coating) were welded by the CMT-Process at the Fronius-technology center. The welding velocity was 60 cm/min with a wire velocity of 3.8 m/min under Argon atmosphere. The thickness of the aluminum sheet was 1.5 mm that of the steel sheet 1 mm. The welding consumables were alloys of AlSi5 and a special solder alloy containing Si and Mn (SSAlSiMn). Figure 4 shows a welding of Al and steel. Table II displays the investigated material combinations.

Table II: Matrix of investigated material combinations by CMT-welding

Sample No.	Solder alloy	Al-sheet-alloy (1.5 mm thick)	Steel-sheet (1 mm thick)
1	AlSi5	AW 5182 (AlMg4.5Mn0.4)	Low C Low Si Low Mn Coated with zinc
2			
3	SSAlSiMn		
4			
5	AlSi5	AW 6181 (AlMg1Si0.8)	
6			
7	SSAlSiMn		
8			

Figure 4 shows a joint between Al- and a steel sheet. Although the IMP cannot be seen, the heat affected zone between solder and Al-sheet is observable.

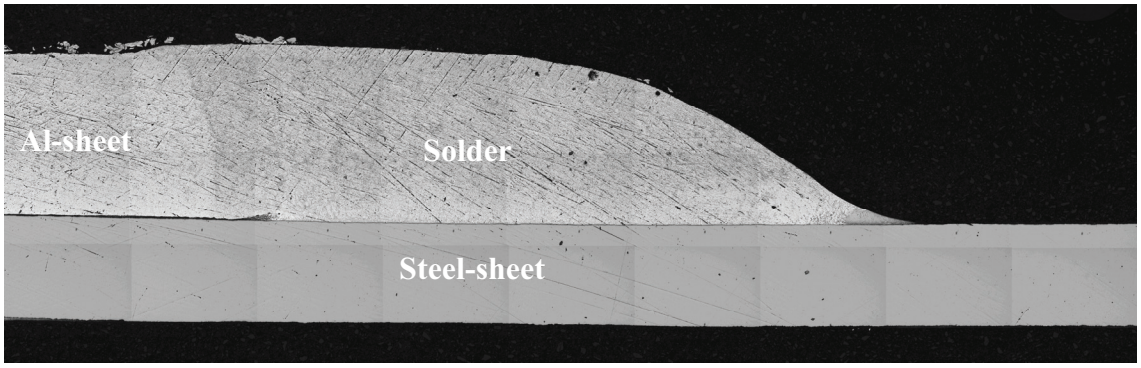

Figure 4: CMT-welding of steel and Aluminum

Results and discussion

The morphology of the IMPs was characterized by metallographic investigations, the chemical composition by SEM-EDX and the hardness by an AFM with a Nanoindenter. The influence of the alloying elements Si, Mn and Zn was calculated using Factsage.

Morphology of the IMP

Figure 5 shows the typical microstructure of the IMP. This phase has an smooth surface at the steel side and a structured surface towards the solder. The average thickness of the IMP is 5.18 µm when using the special alloy SSAlSiMn and 3.47 µm when using the AlSi5 wire. The literature indicates the maximum thickness of a satisfying weld to range at 10 µm. Therefore the CMT-Process allows to use different wire alloys for joining Al and steel .

Chemical composition of IMPs

The chemical composition of the IMPs was quantified by an SEM-EDX at the Department of Metallurgy, University of Leoben. The different Al-sheet-alloys are not influencing the IMP, therefore Table III only shows average compositions of the IMPs of the 6xxx Al-sheet alloy. When using the special alloy a high amount of Si in the IMP was analyzed. The interaction volume of the SEM-EDX analysis was partly bigger than the IMP.
Although the utilization of a focus ion beam (FIB) could have decreased the influence of the solder material, this method was not deployed for economic reasons.

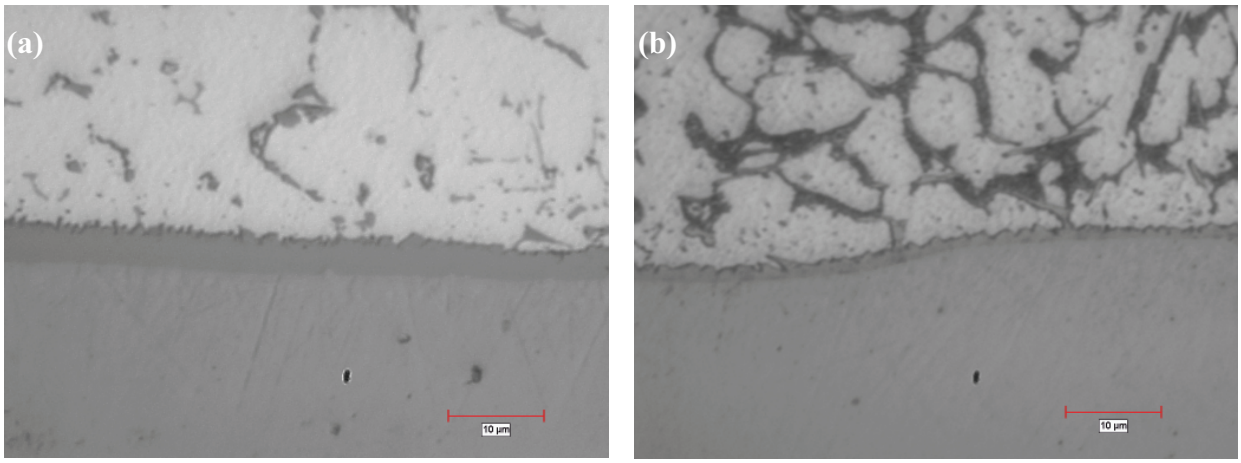

Figure 5: Typical microstructure of CMT-weldings. (a)SSAlSiMn, (b)AlSi5. Magn. 1000

Table III: Average chemical composition of the IMP between steel and solder, Fe balanced, in atomic percent

Sample No.	Al	Si	Mn	Zn
5	60.94	6.80	0.00	1.60
6	60.62	6.01	0.00	1.30
7	60.48	8.35	1.80	2.12
8	61.60	4.87	3.60	1.19

Hardness of IMPs

The conventional method of the measurement of micro hardness did not work for characterizing the IMPs, because the thickness of these phases are less then 10 µm. The experiments were performed on a Hysitron Triboscope, an add-on indentation device, mounted on the scanner head of a DI (Veeco) Dimension 3100 atomic force microscope (AFM). By this combination the indenter tip is scanned across the sample surface whereby a topography image with high resolution can be produced. This enables the operator to choose the area of indentation with an accuracy of down to 20 nm. The indentation device is basically a three-plate capacitor (Figure 6) with a movable centre plate mounted on small springs. Applying a voltage on the outer plates causes a force on the centre plate to which a shaft with a diamond tip at its end is attached, so that the tip is driven into the sample of interest. Simultaneously the displacement of the centre plate causes a change in the capacity, which, after a precise calibration, serves as a measure for the penetration of the tip into the sample.

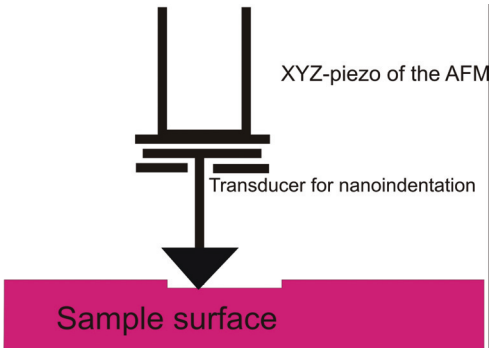

Figure 6: Schematically assembly of the AFM with Nanointender

The primary result is a force-displacement curve (Figure 7)from which, usually using the unloading part of the curve, nanohardness and elastic modulus can be extracted. The most common procedure is the method by Oliver and Pharr which was used also for the present investigation[16]. As diamond tip we used one with a cube corner geometry with the advantage of a small tip radius and therefore a high spatial resolution. Since the key parameter for the evaluation of hardness and elastic modulus from such experiments is the contact area between tip and indented sample surface, the relation between indentation depth and contact area, the so-called area function, was calibrated with great care on a fused quartz standard sample. The resolution (floor noise) in force and displacement of the setup were 1 µN and 0.1 nm, respectively. One loading cycle consisted of five segments with one holding period at a standard maximum load of 1000 µN, in order to let effects like indent creep get finished, and a second holding period for an estimate and eventual correction of thermal drift of the instrument.

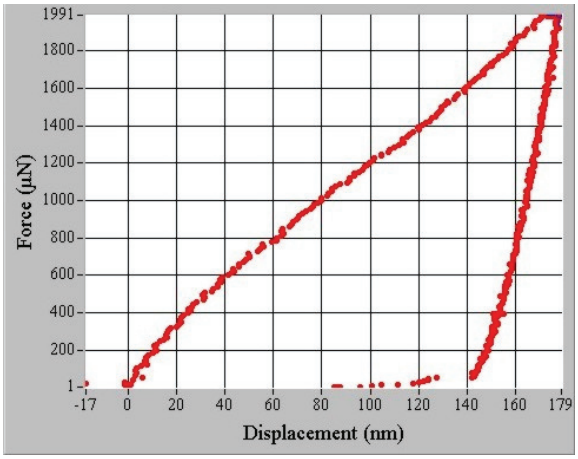

Figure 7: Force-displacement curve as the primary result of the measurement

The absolute values of the measurement do not correspond to values in the literature since different hardness analysis methods were used. Therefore the relative hardness difference between the FeAl-phases was calculated. The Fe_2Al_5- and $FeAl_2$-phases have a higher hardness of 10 to 15 % in contrast to the $FeAl_3$ phase. A pilot survey of crawlers of solder on a steel sheet evinced the $FeAl_3$ in case of the sample 2-23 and an other IMP in the sample 1-9. The IMP with small indents, higher hardness, is depicted in Figure 8. The surrounding material has a deeper indent and consequently a lower hardness than the IMP.
The range of the applicable $FeAl_3$ against the unemployable harder $FeAl_3$ and Fe_2Al_5 was chosen between 12 and 15.5 GPa referring to the preliminary investigations (Table IV). The elastic modulus characterizes the quality of the measurement. The values should be comparable.

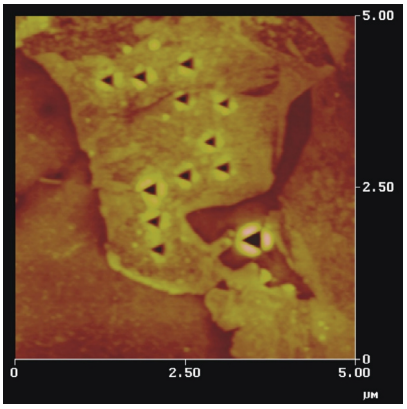

Figure 8: Intends of the measurement with a AFM-Nanoindenter

Table IV: Hardness H and elasticity modulus E of weldings and pilot survey (1-9, 2-23)

	E (GPa)	deviation	H (GPa)	deviation
steel sheet			2.61	
Al sheet (5xxx)			0.96	
1	173.13	6.58	13.26	0.84
2	182.12	9.14	14.10	0.85
3	174.91	5.64	15.13	0.35
4	179.04	6.56	14.38	0.39
1-9	196.97	3.06	16.11	0.48
2-23	167.00	11.07	14.01	0.64

The influence of the alloying elements

The interaction of the alloying elements Mn, Si and Zn is important for the formation of IMPs. The base of the Factsage calculations is the Fe-Al phase diagram (Figure 1). Although the used databases were incomplete concerning IMPs, an influence of these elements could be observed. Another problem is that thermodynamic programs do not take the temperature gradient, solidification velocity and segregations into account.
The following diagrams show the influence of Mn, Si und Zn on the formation of IMPs. The abscise displays the Al content of different FeAl-phases. A slight disagreement can be observed, because of the usage of unequal databases of Factsage.
Mn and Si expand the stability area of the $FeAl_3$ phase and move the stability to a lower Al concentration (Figure 9, Figure 10). The Si database did not include the Fe_2Al_5 phase.

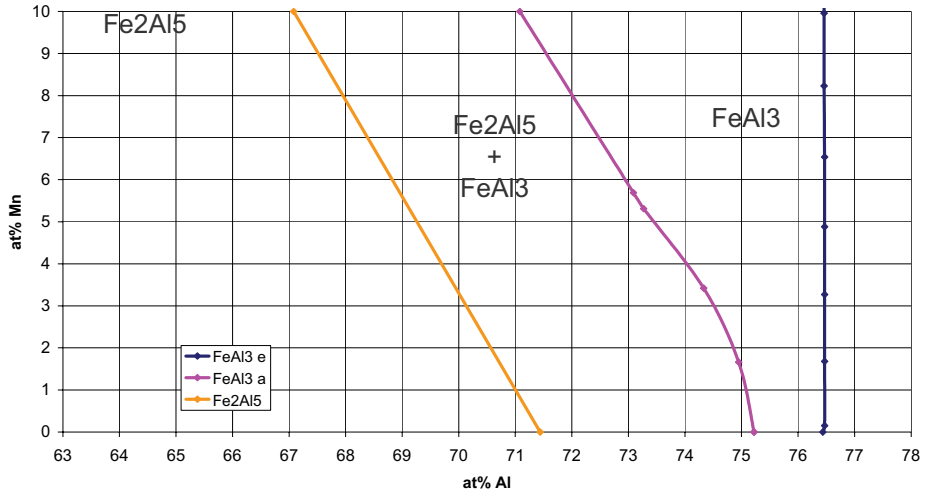

Figure 9: Influence of Mn on the IMP at 300 K. e End, a Begin

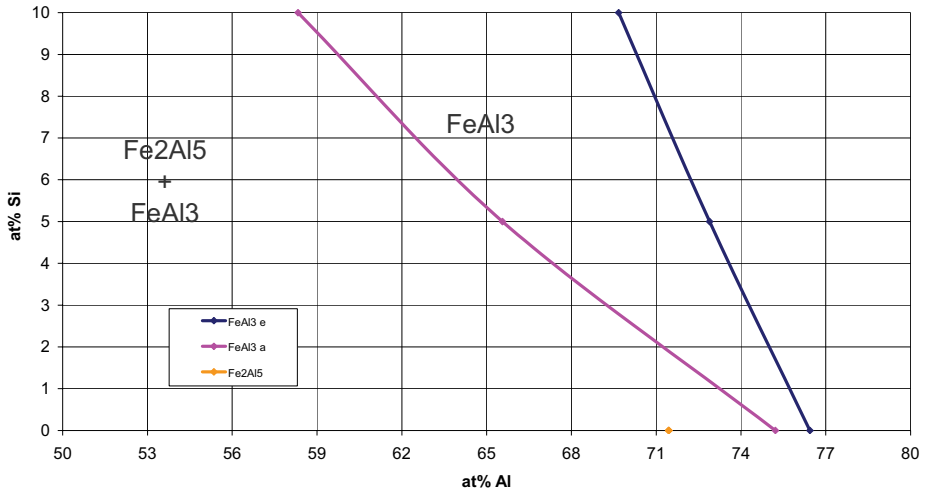

Figure 10: Influence of Si on the IMP at 300 K. e End, a Begin

The influence of the Zn is different. Figure 11 indicates that the IMPs are moved to lower Al concentrations, although the stability area of the $FeAl_3$ was not widened.

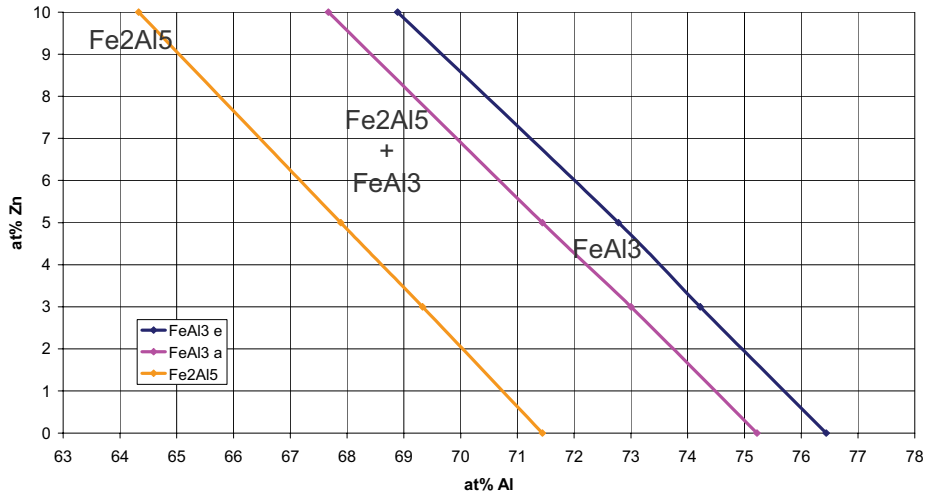

Figure 11: Influence of Zn on the IMP at 300 K. e End, a Begin

Modeling the $FeAl_3$ phase by variation of the alloying elements

Aiming at a quick forecast of the possible formation of IMPs, the modeling of thermodynamic calculations is an important goal. The stability of the $FeAl_3$ phase is analytically derived, including the influencing and interacting elements Mn, Si and Zn. The equations of the Al rich side of the $FeAl_3$ phase is shown in (1) and of the lower Al side in (2).

$FeAl_3$ begin – Al rich

$$\%Al_{NEW}=76.44-(0.02\cdot\%Mn+0.68\cdot\%Si+0.76\cdot\%Zn) \quad (1)$$

$FeAl_3$ ends – lower Al concentration

$$\%Al_{NEW}=75.22-(0.42\cdot\%Mn+1.87\cdot\%Si+0.76\cdot\%Zn) \quad (2)$$

Conclusion

An advanced joining process was developed, which provides several advantages concerning process stability and mechanical properties of the produced compounds.
Fronius International Ltd. authorized the Nonferrous Metallurgy Department, University of Leoben, Austria, to investigate their new joining method of Al and steel to characterize the formed IMP.
The morphology and the thickness of the IMPs correlate with the content of the alloying elements Si, Mn and Zn. The IMP is thicker when using the solder alloy SSAlSiMn than when using AlSi5. The lower Si content is responsible for this effect.
The influences of the alloying elements Mn, Si and Zn are nearly the same. All of these elements move the thermodynamic equilibrium of the IMPs $FeAl_3$ and Fe_2Al_5 to lower Al concentrations. Mn and Si expand the stability area of the $FeAl_3$ phase. The Zn databases were empty or not optimized.
As a result of the thermodynamic calculations and the usage of an AFM with Nanoindenter, the $FeAl_3$ IMP has been characterized. During these investigations the Fe_2Al_5, which has an unacceptable toughness, was not found. The CMT-Process forms the ductile $FeAl_3$ phase by using a solder alloy like SSAlSiMn or AlSi5.
The joining of thin Al- and steel sheets is important for a continuous economic production and use in the automotive industry. However investigations concerning the corrosion behavior between Al and steel welds should be investigated. It can be said that Mn acts in a positive manner against corrosion.
Simulation is an important tool for the future during the development of new joining technologies and characterization of formed phases. Therefore, it is necessary to increase the contents of thermodynamical databases concerning high amounts of alloying elements.

References

[1] W. Beyer, Schweißtechnik Berlin, (1969), 179-183
[2] H.M. Ghanam, PhD Thesis, RWTH Aachen, (1968)
[3] M.J. Rathod, M. Katsuna, Welding Journal, January (2004), 16-26
[4] J. Resch, PhD. Thesis, Leoben (1994)
[5] Metals Handbook, Vol. 63, 10th Edition, ASM International, (1992)
[6] R.W. Richard, et al., International Material Revue 39 (5) (1994) 191
[7] Bulletin of Binary Phase Diagrams, ASM International, (1994)
[8] I.D. Maruin, Revue. Metallurgy 22, (1925), 139
[9] M. Agiew, O.L. Viwr, Journal Inst. Met. 44, (1930), 89
[10] E. Gebhardt, W. Obrowski, Zeitschrift Metallkunde. 44, (1953), 154
[11] V.N. Yermenko, et al., Journal of Material Science. 16 (9), (1981), 1748-1756
[12] G. Eggeier, W. Auer, H. Kaesche, Journal of Material Science 21 (9), (1986), 3348
[13] A. Bahadur, O.N. Mohanty, Material Transaction, JIM 32 (11), (1991), 1053
[14] A. Bahadur, O.N. Mohanty, Material Transaction., JIM 36 (9), (1995), 1170
[15] K. Bouche, et al., Material Science Engineering A 249, (1998), 167
[16] Oliver, Pharr, Journal Mater, Res. 7 (1992), 1564